A wavelet-based method to measure the toroidal mode number of ELMs

Francesca M. Poli[1)], Sergei E. Sharapov[2)] and JET-EFDA contributors[a)]

JET-EFDA, Culham Science Centre, OX14 3DB, Abingdon, UK

[1)] *University of Warwick, Coventry CV4 7AL, UK*

[2)] *EURATOM/UKAEA Fusion Assoc., Abingdon OX14 3DB, UK*

[a)] *See the Appendix of F. Romanelli et al., Fusion Energy 2008 (Proc. 22nd Int. Conf. Geneva, 2008) IAEA, (2008)*

(Received: 5 September 2008 / Accepted: 2 December 2008)

The high confinement mode regime (H-mode) in tokamaks is accompanied by the occurrence of burst of MHD activity at the plasma edge, so-called edge localized modes (ELMs). Because of the short time scales involved in the ELM crash (on JET typically 0.2 ms), standard Fourier analysis can hardly be used to extract their toroidal mode number. On the other hand, the assessment of linear stability of ELMs with the ion drift effects included, makes the identification of their toroidal mode numbers an important issue, while an accurate comparison with the theory of nonlinear evolution of ELMs requires the knowledge of the nonlinear spectrum. Compared to Fourier analysis, wavelets are suitable to study transient events on time scales comparable to the wave period. Spectral analysis based on sinusoidal wavelet functions has been applied to study the spectral properties of magnetic perturbations associated with ELMs and with their precursors, in JET plasmas with toroidal rotation driven by unbalanced NBI. It is shown that, combining wavelet analysis with statistical two-point correlation techniques, it is possible to get information on the toroidal mode number structure of magnetic perturbations during the phases that immediately precede the ELM and during the ELM crash itself.

Keywords: ELMs, precursors, toroidal mode number, wavelets

1. Introduction

The high confinement regime mode (H-mode) in tokamaks is accompanied by the occurrence of bursts of MHD activity at the plasma edge, so-called edge localized modes (ELMs). On the JET tokamak ELMs last typically during 0.2 ms and are often preceded by coherent magnetic oscillations, the ELM precursors, whose toroidal mode number, inferred from the phase shift of magnetic perturbations, is $n < 15$ [1]. The existence of magnetic precursors is confirmed in most tokamaks, with lifetime varying between fractions and hundreds of ms, and frequency spanning in a range of a few kHz to hundreds of kHz (see, for example the review papers by Zohm [2] and Kamiya [3] for an overview of ELM properties based on experimental observations). The identification of ELM precursors and post-cursors is a well assessed problem, since their spectral features, amplitude, frequency, toroidal and poloidal mode number, can be extracted from the time series of magnetic perturbations using standard analysis based on Fourier techniques. This is not the case for the spectral features of ELM themselves, because the short time scales involved in the ELM crash make it difficult to extract their mode number and frequency structure. It is today generally accepted that type-I ELM are coupled peeling-balloning instabilities [4]. The assessment of linear stability of ELMs with the ion drift effects included, makes the identification of their toroidal mode numbers an important issue [5], while an accurate comparison with the theory of nonlinear evolution of ELMs [6] requires the knowledge of the nonlinear spectrum. Compared to Fourier analysis, wavelets are suitable to study transient events on a time scale comparable to the sampling rate, which is 1μs in the case of magnetic coils on JET. Wavelet analysis represents a step-forward in the identification and spectral characterization of short-lived coherent precursors, since allows to study the temporal evolution of amplitude, frequency and mode number over time scales comparable with the wave period [7][8]. Contrary to the case of ELM precursors and post-cursors, described in [8], where the number of modes is limited to one or two and their spectral features change over scales longer than the wave period, in the case of the ELM themselves the wavelet spectrum is of difficult interpretation. This is discussed in this paper, where it is shown that, combining the wavelet coefficients with the two-point correlation technique developed by Beall et al [9], the coherent part of the ELM spectrum is enhanced with respect to the incoherent background. The properties of wavelets compared to short-time Fourier analysis are reviewed in Sec. 2. The measurement of the toroidal mode number of ELMs is discussed in Sec. 3 in a case study, a type-I giant ELM on JET. Conclusions and future directions are addressed in Sec. 4.

2. Method

Spectral analysis of plasma fluctuations is traditionally based on Fourier analysis. The hypothesis behind is that fluctuations may be regarded as the superposition of independent, sinusoidal waves, with frequency ω and wavenumber k. Whenever fluctuations are stationary over

author's e-mail: f.m.poli@warwick.ac.uk

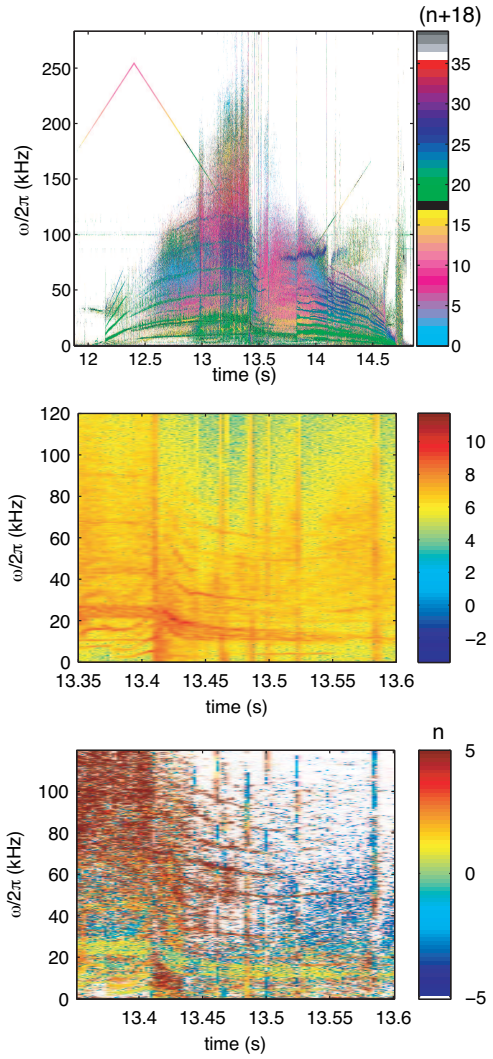

Fig. 1 JPN 42976. (a) toroidal mode numbers. (b) power spectrum in a time window centered on the type-I giant ELM. (c) toroidal mode number calculated from two edge coils separated by 10.17 degrees. Color scales are saturated, modes with $|n| > 5$ are deep red.

a time window of length T, they can be represented as the superposition of sinusoidal modes over the interval T. Fourier analysis is routinely used on JET to study the spectra of MHD instabilities and turbulence, including their toroidal and poloidal mode number structure. An example is shown in Fig. 1 in the case of a D-T plasma discharge on JET, shot number #42976, with 16.1 MW of fusion power [10]. Figure 1(a) shows the time evolution of the toroidal mode number of magnetic fluctuations, measured with a set of Mirnov coils located at the plasma edge, at major radius $R = 3.884$ m, $z = 1.03$ m above the midplane, and separated along the toroidal direction by 10.17 degrees [11]. The power spectrum in a time window centered on the type-I giant ELM at 13.41 s, is shown in Fig. 1(b). The time dependent spectrum is defined as the squared value of the short-time Fourier Transform (STFT) $S_{m,k}$ [12]:

$$S_{m,k} = \sum_{l=0}^{N-1} x[l]\, g[l-m] e^{-\imath 2\pi k l/N} \tag{1}$$

where $\{x[l]\}$ is the discrete time series of magnetic perturbations, acquired at the sampling rate of $t_s^{-1} = 1$ MHz, with discrete frequency components $\omega_k = \pi k/Nt_s$ $(k = 1, \cdots N)$ and $g[l-m]$ is a symmetric window, centered at times $t[m] = mt_s$. The minimum nonzero frequency that can be measured is π/Nt_s and depends on the number of points used to compute the Fourier Transform, i.e. on the window length $T = Nt_s$, while the maximum resolvable frequency, the Nyquist frequency $\omega_N = \pi/t_s$ depends only on the acquisition time. The STFT has been computed over time windows of 4 ms length, with a 50% overlapping to each other. The corresponding separation between frequency components is therefore ~ 0.25 kHz, large enough to resolve significant spectral components associated with coherent, slow-varying coherent modes. Generally speaking, the computation of the STFT of a time series requires N points, where the value of N is chosen in order to optimize the time-frequency resolution. The resulting power spectrum is an average of the spectral components over the time window $T = Nt_s$. The time averaging that is implicit in the definition of the Fourier Transform makes therefore it difficult to detect variations in spectral quantities that occur over time scales shorter than T. This is the case for short-lived ELM precursors and post-cursors, as well as for the ELMs themselves. In the latter case, in fact, the typical time scales for an ELM crash are 0.2 ms on JET, much shorter than the time scales available to Fourier analysis. As shown in Fig. 1(c), a toroidal mode number cannot be assigned to ELMs on the basis of a Fourier phase-spectrogram. The color coding is confused in time windows where ELMs occur and a coherent phase shift cannot be identified.

Significant advantages in the study of the spectral features of short-lived coherent modes are introduced by the use of wavelet functions, as discussed in [8]. Not only precursors with lifetime shorter than 1 ms are easily detected in the wavelet spectrum, but the time evolution of their amplitude, frequency and toroidal mode number can be followed with a time resolution comparable to the wave period. In addition, due to the lower noise level typical of the wavelet transform, the determination of n's is much less affected by random phase oscillations. We analyze the spectra of magnetic perturbations using the Morlet wavelet, a sinusoidal function modulated by a Gaussian envelope (see, for example Ref. [13]):

$$\psi(t) = \pi^{-1/4} e^{-t^2/2} e^{\imath 2\pi t} \tag{2}$$

This choice is dictated by the fact that the Morlet wavelet is suitable for the study of spectral features, such as the amplitude, frequency and phase shift, of transient events. The Morlet wavelet has clear similarities with Fourier eigenmodes, which are localized in times. The continuous

wavelet transform (CWT) of a discrete time series $\{x[l]\}$, sampled at the rate t_s, is defined as the convolution product of $\{x[l]\}$ with a scaled ($t \rightarrow t/s$) and shifted ($t \rightarrow t - \tau$) version of $\psi(t)$:

$$W_m(s) = \sum_{n=0}^{N-1} x[l]\psi^*\left(\frac{n-m}{s}t_s\right) \tag{3}$$

Apart from the normalization factors, the only difference between (3) and the STFT is that the windowing is intrinsic in the wavelet transform and it depends on scale s. Using the property that the Fourier Transform of a convolution product between two functions is the product of the Fourier Transforms of the functions themselves, the wavelet transform $W_m(s)$ can be efficiently computed as an inverse Fourier Transform [14]:

$$W_m(s) = \left(\frac{2\pi s}{t_s}\right)^2 \sum_{k=0}^{N-1} \hat{x}[k]\hat{\psi}_0^*(s\omega_k)e^{i\omega_k m t_s} \tag{4}$$

where $\hat{x}[k]$ is the Fourier transform of the time series and $\hat{\psi}_0(s\omega_k)$ is the normalized Fourier Transform of the Morlet wavelet (2):

$$\hat{\psi}_0(s\omega_k) = \pi^{-1/4}H(\omega)e^{-(s\omega-\omega_0)^2/2} \tag{5}$$

where $\omega_0 = 2\pi$ in our case and $H(\omega)$ is the Heaviside step function, with $H(\omega) = 1$ for $\omega > 0$ and $H(\omega) = 0$ otherwise. The wavelet transform has been computed using the Fast Fourier Transform algorithm, at scales $s = s_0 a^j$, where s_0 is the minimum available scale and, for each value of j, $a = 2^{-\nu}$ provides a refining of scales in each *octave* $(2^j, 2^{j+1}]$ [12].

3. Results

We have computed the wavelet coefficients from the time trace of magnetic perturbations measured by two pairs of edge Mirnov pickup coil located at $R = 3.884$ m, $z = 1.013$ m over the equatorial plane, and toroidally separated. Two coils are 10.17 degrees apart, allowing the measurement of toroidal mode numbers up to 15, the second pair has mutual separation of 5.63 degrees and allows the measurement of toroidal mode numbers up to 30.

Figure 2 shows the wavelet scalogram (the equivalent of spectrogram with frequencies replaced by scales) computed from (4) in the case of pulse #42976, in a time window centered on the ELM. The ELM precursor, an external kink mode [5], is indicated in the wavelet scalogram as the coherent mode that starts from $t \sim 13.37$ s and whose frequency increases with time. The ELM is seen in the wavelet scalogram as a structure that extends from low to high frequencies. The distortion in the spectrum at large scales, typical for continuous wavelet transforms [12], mask low frequency spectral features; we therefore discard spectral components at scales larger than $\log_2(s) = 12$, corresponding to frequencies below 1 kHz, in our discussion. The toroidal mode number can be inferred

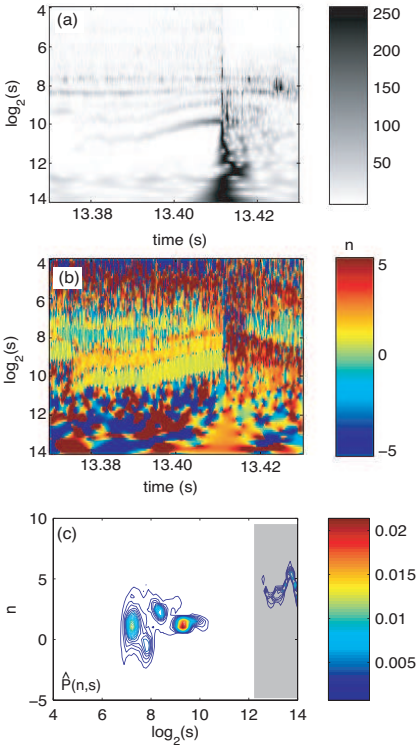

Fig. 2 JPN 42976. (a) Normalized wavelet coefficients. (b) toroidal mode number. (c) Normalized spectrum $\hat{P}(n, s)$, computed from the wavelet coefficients in the time window between 13.37 s and 13.41 s.

from the phase shift between two Mirnov coils divided by their toroidal separation as:

$$n = \frac{1}{\Delta\phi}\arg[W_m^*(\phi_1, s)W_m(\phi_2, s)] \tag{6}$$

and it is shown in Fig. 2(b). While the toroidal mode number of the precursor is easily identified in the phase spectrogram, the toroidal mode number get confused in the plot when approaching the ELM and it is difficult to drive any conclusion. The phase shift undertakes jumps of 2π right before the ELM crash and coherent modes spread in toroidal mode number. In order to better visualize the range of toroidal mode numbers involved during the phases that immediately precede the ELM, and during the ELM burst itself, we have applied a statistical analysis based on a two-point correlation technique [9]. After having computed the wavelet coefficients from (4), we have constructed the mode number and frequency spectrum $P(n, s)$ as follows:

$$P(n, s) = \frac{1}{N}\sum_{j=1}^{N} I_\Delta[n^j - \bar{n}]P(s) \tag{7}$$

where $P(s) = 0.5 \times [P_1(s) + P_2(s)]$ is the average of the power spectra measured at positions ϕ_1 and ϕ_2, respectively. The average is introduced only to have more statistics, since we could have used either $P_1(s)$ or $P_2(s)$ with

minimal differences in the final results. The toroidal mode number n^j is computed from the wavelet coefficients, using Eq. (6), with the index j running over time. The indicator function I_Δ, the discrete equivalent of the delta function, is defined as:

$$I_\Delta[n^j - \bar{n}] = \begin{cases} 1 & \bar{n} - \Delta \leq n^j < \bar{n} + \Delta \\ 0 & elsewhere \end{cases} \quad (8)$$

Computing (7) is equivalent to constructing a histogram. For each time step $t_j = jt_s$, the value of the toroidal mode number n^j is compared with the reference values of $\bar{n} = [-30, 30]$. The bin width has been chosen equal to $\Delta = 0.5$ cm^{-1}, in order to minimize the variance of the power spectrum estimate. The outcome is a robust estimate of the frequency- wavenumber power spectrum [16]. Following [9] we define the conditional spectrum, $P(n|s) = P(n,s)\left[\sum_s P(n,s)\right]^{-1}$, which can be interpreted as the probability that a mode measured at frequency s^{-1} has toroidal mode number n. Figure 2(c) shows the normalized spectrum $\hat{P}(n,s) = P(n,s)[\sum_{s,n} P(n,s)]^{-1}$ computed in the time window between 13.37 s and 13.41 s. During this phase the dominant contribution to the total power spectrum is given by the ELM precursor and its harmonics, represented in the plot as 'spots' with toroidal mode number $n = 1, 2, 3$ and $\log_2(s)$ between 6 and 10. As shown in Fig. 2(a), the measured frequency of the precursor increases (i.e. the wavelet scale decreases), as well as the amplitude of the fundamental harmonics. The contribution to the total power spectrum is therefore larger in the latest time phase, approaching the burst. Figure 3 shows $P(n,s)$ and $P(n|s)$ computed in two time windows. The first window $t = [12.4110, 12.4112]$ s corresponds to the 200 μs that precede the ELM, while the second window, $t = [12.4112, 12.4116]$ s covers the ELM burst, which coincides with the phase when the D_α emission rapidly increases. Since the phase undertakes jumps of 2π in these windows, we have computed the toroidal mode number from the pair of Mirnov coils with the smaller toroidal separation, $\Delta\phi \sim 5.63$ degrees. The results of the analysis coincide with the results obtained from the pair with larger toroidal separation in frequency ranges where the phase variations are smooth, but are less affected by phase jumps during the ELM crash. From a comparison between Fig. 2(c) and Fig. 3(a) we can see that the toroidal mode number structure changes during the phases that immediately precede the ELM. During the 200-300 μ that precede the burst, the maximum contribution to the total power spectrum comes from spectral components with low toroidal mode number, $n = 1, 2$ and frequencies lower than that of the precursor [$\log_2(s) > 10$]. These components also have a smooth variation in the toroidal mode number, which tends to increase in absolute value, as it is made more evident in the conditional spectrum, Fig. 3(b). A jump in the phase is measured at $\log_2(s) \sim 12$, although we remind that spectral components with scale larger than this value are not discussed herein.

As shown in Fig. 3(b), spectral components with logarithmic scale between 6 and 7 have toroidal mode numbers regularly distributed between ±10, while at smaller scales, namely frequencies larger 100 kHz, the toroidal mode number is spread between ±30, with no clear trend. In this frequency range the power spectral density is low and mode phase have poor correlation. During the ELM crash, the toroidal mode number measured in the range of scales where the precursor is detected, with [$\log_2(s) = 8$ to 10, evolves towards even larger values, up to 25. The spectrum at lower frequencies stays almost unaffected, with toroidal mode numbers low in value, while the spectrum at larger frequencies develops a more clear structure, with definite frequencies associated with definite toroidal mode numbers. We cannot exclude that the toroidal mode number in this range of frequencies may be even larger than those measured here and that these apparent trends at high frequency are partly due to an aliasing effect. The measured range of n values suggest that the ELM instability has a ballooning character. The evolution of toroidal mode number towards larger values has been predicted by ideal MHD theory [17], although the simulations in that case were done assuming that the ELM precursor was a ballooning instability with $n \sim 5$, while in this case the precursor is an external kink mode. Evidence for increasing in the toroidal mode number were also derived from target load pattern on ASDEX-U where, in the start phase of the ELM collapse is $n \sim 3 - 5$, evolving to values of $n \sim 12 - 14$ during the ELM power deposition maximum [18].

4. Conclusions

An approach is suggested for determining toroidal mode numbers of ELMs, suitable for the short time scales involved in the ELM dynamics. The technique, commonly used to recover the dispersion relation of waves in plasmas [16], consists of a wavelet analysis, which provides good resolution in time, supplemented by a two-point correlation technique, which provides a robust statistical reconstruction of toroidal mode numbers involved in an ELM event. Using a wavelet-based two-point correlation, the coherent part of the ELM spectrum is enhanced, while the incoherent part is averaged out giving negligible contribution to the total spectrum. The application of the method to H-mode plasma discharges with type-I ELMs on JET indicates that spectra with statistical significance can be obtained over time windows of 50 μs length. It is found that the toroidal mode number of a type-I giant ELM, observed in a D-T plasma discharge starts from low toroidal mode numbers, consistently with the toroidal mode number of the precursor, an external kink mode with $n = 1$ [5]. The toroidal mode number increases approaching the ELM and a broad range of values, from 1 to 30 are measured during the burst, indicating that the ELM consists of the superposition of many modes. Preliminary analysis over H-mode type-I ELMs confirm these results, indicating

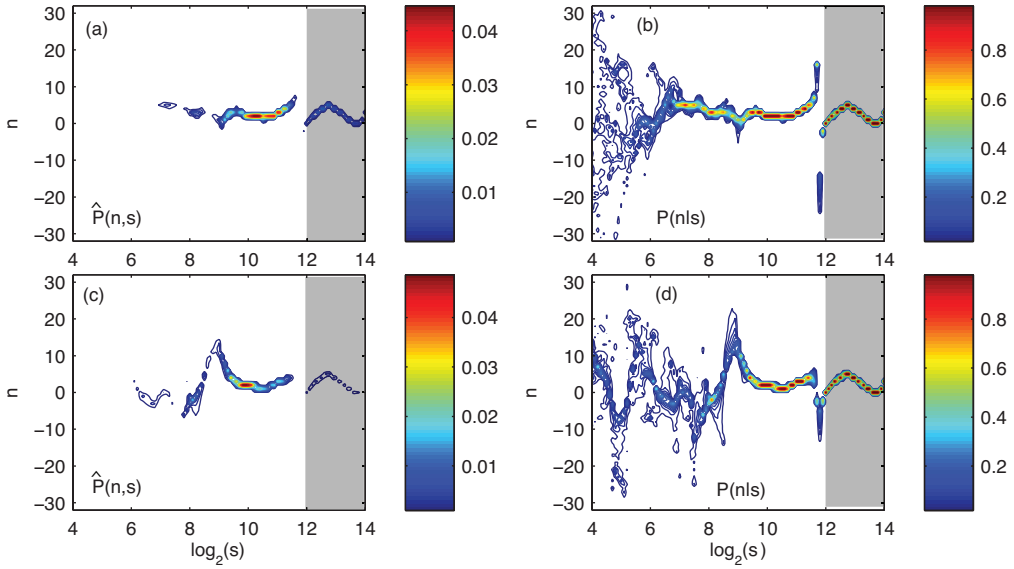

Fig. 3 (a) Normalized spectrum $P(n, s)$, computed from the wavelet coefficients in the time window $t = [12.4110, 12.4112]$ s, before the ELM crash. (b) Conditional spectrum, in the same time window. (c)-(d) Same as (a) and (b) but during the ELM, between 12.4112 s and 12.4116 s. Shaded areas indicate the range of scales that is discarded in the discussion.

that the toroidal mode number of an ELM increases immediately before the burst, although the maximum value may vary depending on the background plasma. Deeper analysis over a set of JET discharges is ongoing, including the cases of ELMs triggered by pellets and ELMs mitigated by Error Field Correction Coils.

This work has been conducted under the European Fusion Development Agreement. The views and opinions expressed herein do not necessarily reflect those of the European Commission. F M. Poli is funded by the UK EPSRC.

[1] Perez C. P, Koslowski H. R, Huysmans G. T. A, *et al*, Nucl. Fusion, **44**, 609 (2004).
[2] Zohm M, Plasma Phys. Control. Fusion, **38**, 105 (1996).
[3] Kamiya K, Asakura N, Boedo J, et. al, Plasma Phys. Control. Fusion, **49**, S43 (2007).
[4] Connor J. W, Plasma Phys. Control. Fusion, **40**, 191 (1998). *Ibid*, **40**, 531 (1998)
[5] G T A Huysmans, S E Sharapov, A B Mikhailovskii and W Kerner, Phys. Plasmas **8**, 4292 (2001).
[6] H.R. Wilson and S.C. Cowley, Phys. Rev. Lett. **92**, 175006 (2004).
[7] T Kass, S Günter *et al*, Nucl. Fusion, **38** 111 (1998).
[8] F M Poli, S E Sharapov, S C Chapman *et al*, Plasma Phys. Control. Fusion, **50** 095009 (2008).
[9] J. M. Beall, C. Kim, and E. J. Powers, J. Appl. Phys. **53**, 3933 (1982).
[10] M Keilhacker, Nucl. Fusion **39**, 209 (1999).
[11] R. F. Heeter, A. F. Fasoli, S. Ali-Arshad, and J. M. Moret, Rev. Sci. Instrum., **71** 4092 (2000)
[12] S Mallat, A wavelet tour of signal processing, chapter 4. Academic Press, Cambridge, (2001).
[13] A I Eriksson, Spectral analysis, in Analysis Methods for Multi-Spacecraft Data, ISSI Scientific Report, G Paschmann and P W Daly (Eds), ISSI, Bern (1998)
[14] C Torrence and G P Compo, Bulletin of the American Meteorological Society, **79** 61 (1998)
[15] R. Koslowski et al., Nucl. Fusion **45**, 201 (2005).
[16] T. Dudok de Wit, V V Krasnosel'skikh, *et al*, Geoph. Res. Lett. 22, 2653, 1995.
[17] G T Huysmans *et al*, Proceedings of the 35th EPS Plasma Physics Conference, Hersonissos, Crete, Greece, (2008).
[18] T Eich, A Herrmannm J Neuhauser *et al*, Plasma Phys. Control. Fusion **47** (2005) 815.